

Receptor arrays optimized for natural odor statistics

David Zwicker,^{1,2,*} Arvind Murugan,^{3,†} and Michael P. Brenner^{1,2,‡}

¹*School of Engineering and Applied Sciences, Harvard University, Cambridge, MA 02138, USA*

²*Kavli Institute for Bionano Science and Technology,
Harvard University, Cambridge, MA 02138, USA*

³*Department of Physics and the James Franck Institute, University of Chicago, Chicago, IL 60637, USA*

(Dated: January 12, 2016)

Natural odors typically consist of many molecules at different concentrations. It is unclear how the numerous odorant molecules and their possible mixtures are discriminated by relatively few olfactory receptors. Using an information-theoretic model, we show that a receptor array is optimal for this task if it achieves two possibly conflicting goals: (i) each receptor should respond to half of all odors and (ii) the response of different receptors should be uncorrelated when averaged over odors presented with natural statistics. We use these design principles to predict statistics of the affinities between receptors and odorant molecules for a broad class of odor statistics. We also show that optimal receptor arrays can be tuned to either resolve concentrations well or distinguish mixtures reliably. Finally, we use our results to predict properties of experimentally measured receptor arrays. Our work can thus be used to better understand natural olfaction and it also suggests ways to improve artificial sensor arrays.

Discrimination of olfactory signals occurs in a high-dimensional space of odor stimuli in which a large number of distinct molecules and their mixtures can be distinguished by a much smaller number of receptors [1–3]. For example, humans have about 300 distinct olfactory receptors [4], which can sense at least 2100 odorant molecules [5] and the real number might be much larger [1]. Moreover, humans can differentiate between mixtures of up to 30 odorants [6]. Such remarkable molecular discrimination is thought to use a combinatorial code [7, 8], where typical odorant molecules bind to receptors of multiple types [1, 3]. Each receptor type is expressed in many cells [9] and the information from all receptors of the same type is accumulated in corresponding glomeruli in the olfactory bulb [10], see Fig. 1A. The activity of a single glomerulus is thus the total signal of the associated receptor type, so the information about the odor is encoded in the activity pattern of the glomeruli [11]. This activity pattern is interpreted by the brain to learn about the composition and the concentration of the inhaled odor. We here study how receptor arrays can maximize the transmitted information.

It is known [12, 13] that the input-output characteristics of sensory apparatuses of many organisms are tailored to the statistics of the organism’s natural environment to maximize information transmission. For example, in the visual circuit of the fly, the input-output relationship of neurons is matched to the cumulative distribution of the input distribution [12]. Similar observations have since been made in many sensory systems [13, 14] and even in transcriptional regulation [15]. In

all these cases the distinguishable outputs of the sensory system must be dedicated to equal parts of the input distribution, which is known as Laughlin’s principle [12] or histogram equalization [16]. Intuitively, more of the response range is dedicated to common stimuli, at the expense of less frequent stimuli [12].

Similarly, the binding affinities of olfactory receptors might reflect the natural statistics of odors in an organism’s environment. Odors vary across environments and differ in both their frequency and composition [17]. For example, some molecules might frequently appear together because they originate from the same source while others are rarely found in the same odor. Additionally, some odors are more important to recognize than others, which corresponds to considering an increased frequency for these odors. Together, the frequencies and correlations constitute the natural *olfactory scene*.

It is not clear how olfactory receptors can account for natural odor statistics. Merely dedicating more receptors to common odors is not optimal, given the small number of available receptors and the many-to-many relationship between receptors and odors. Further, the value of a receptor is strongly dependent on how it complements the other receptors in the array; many ‘good’ receptors can still create a poor array. Finally, the concentrations of molecules composing an odor can vary widely. Odors need to be distinguished both in quality and quantity; hence receptors must vary both in what molecules they respond to and how strongly they do this. Given the statistics of an olfactory scene, what combination of odorants should different receptors in an array respond to?

We use an information-theoretic approach to quantify how well a receptor array is matched to given odor statistics. We generalize Laughlin’s principle to the high-dimensional case and show that optimal receptor arrays should obey two general principles:

1. Each receptor should be active half the time when

*Electronic address: dzwicker@seas.harvard.edu; URL: <http://www.david-zwicker.de>

†Electronic address: amurugan@uchicago.edu

‡Electronic address: brenner@seas.harvard.edu

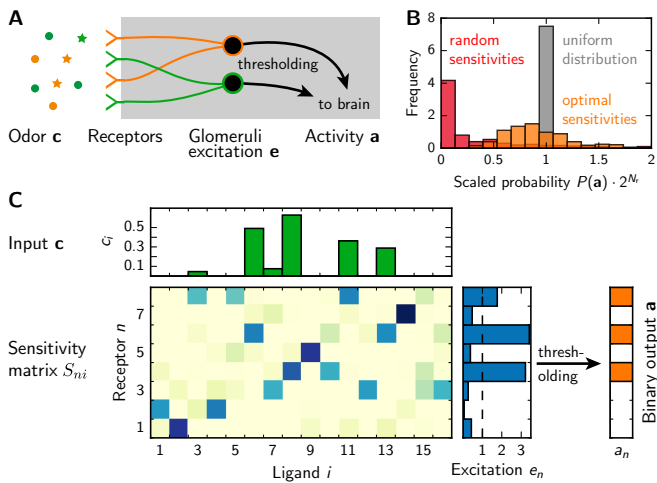


FIG. 1: (A) Schematic representation of the olfactory system, where ligands bind to receptors, whose excitation is accumulated in glomeruli, thresholded, and relayed to the brain. (B) Histogram of the probabilities $P(\mathbf{a})$ of the 2^{N_r} output patterns \mathbf{a} for a random receptor array (red, entropy $I = 6.15$ bits), a numerically optimized one (orange, $I = 7.83$ bits), and the theoretical optimum of a uniform distribution (green, $I = 8$ bits). (C) Schematic representation of our physical model, where the input \mathbf{c} (green bars) is mapped to excitations (blue bars), which are turned into the output \mathbf{a} (orange) by thresholding. Parameters in (B) and (C) are $N_r = 8$, $N_l = 16$, $p_i = \frac{1}{4}$, and $\mu_i = \sigma_i = 1$.

odors are presented with natural statistics.

2. The activities of any pair of receptors should be uncorrelated when averaged over all odors presented with natural statistics.

If both conditions are satisfied for an array of N_r receptors with binary readouts, all 2^{N_r} activity patterns are equally likely when odors are presented with natural statistics, see Fig. 1B. However, these conditions are usually not simultaneously satisfiable. We thus also determine the relative costs of violating the two conditions and use this to carry out numerical and analytical optimizations to determine conditions for optimal receptor arrays.

After introducing our general framework below, we first discuss general properties of optimal receptor arrays. We then consider two different classes of natural statistics, for which we find optimal receptors in terms of random matrices. Here, our information-theoretic approach provides a combined measure of the array's performance in multiple aspects – from the resolution of ligand concentrations to the discrimination of mixture composition. We thus finally discuss the trade-off between such potentially mutually exclusive goals and compare our results to experimentally measured receptor arrays.

I. RESULTS

Odors are mixtures of odorant molecules that are ligands of olfactory receptors. Any odor can be described by a vector $\mathbf{c} = (c_1, c_2, \dots, c_{N_l})$ that specifies the concentrations of all N_l possible ligands. During a single sniff, the ligands in the odor \mathbf{c} come in contact with the N_r different odor receptors. In the simplest case, the sensitivity of receptor n to ligand i can be described by a single number S_{ni} and the total excitation e_n of receptor n is given by [18, 19]

$$e_n = \sum_i S_{ni} c_i. \quad (1)$$

Typical receptors have a non-linear dose-response curve [20] and the output a_n is thus a non-linear function of e_n . Moreover, receptors are subject to noise [21], e.g., from stochastic binding, which limits the number of distinguishable outputs. To capture both effects, we consider receptors with only two output states, which corresponds to large noise [22]. In this case, the activity a_n of receptor n is given by

$$a_n = \begin{cases} 0 & e_n < 1 \\ 1 & e_n \geq 1 \end{cases}, \quad (2)$$

i.e., the receptor is active if its excitation e_n exceeds a threshold. Eqs. 1–2 describe the mapping of the odor \mathbf{c} to the activity pattern $\mathbf{a} = (a_1, a_2, \dots, a_{N_r})$, where the receptor array is characterized by the sensitivity matrix S_{ni} , see Fig. 1C. This activity pattern is then analyzed by the brain to infer the odor \mathbf{c} . Such a distributed representation of odors in activity patterns has been compared to compressed sensing [23]; here we focus on how this representation can be tuned to match the structure of natural odors.

We assume that the structure of natural odors in a given environment can be captured by a probability distribution $P_{\text{env}}(\mathbf{c})$ from which odors are drawn. $P_{\text{env}}(\mathbf{c})$ can encode, for example, the fact that some ligands are more common than others or that some ligands are strongly correlated or anti-correlated in their occurrence. Since natural odor statistics are hard to measure [17], we work with a broad class of distributions $P_{\text{env}}(\mathbf{c})$ characterized by a few parameters. We define p_i to be the probability with which ligand i occurs in a random odor. The correlations between the occurrence of ligands are captured by a covariance matrix p_{ij} . We expect p_i to be small since any given natural odor typically contain tens to hundreds of ligands [19, 24], which is a small subset of all $N_l \gtrsim 2100$ ligands [17]. When a ligand i is present, we assume its concentration c_i has mean μ_i and standard deviation σ_i . Thus, the full natural odor statistics $P_{\text{env}}(\mathbf{c})$ are parameterized by p_i , μ_i , and σ_i for all ligands i and a covariance matrix p_{ij} in our model.

A. Optimal receptor arrays

An optimal receptor array must tailor receptor sensitivities S_{ni} so that the odors-to-activity mapping given by Eqs. 1–2 dedicates more activity patterns to more frequent or more important odors as specified by $P_{\text{env}}(\mathbf{c})$. In information-theoretic terms, the array must maximize the mutual information $I(\mathbf{c}, \mathbf{a})$ [25]. In our model, the mapping from \mathbf{c} to \mathbf{a} is deterministic and I can be written as the entropy of the output distribution $P(\mathbf{a})$,

$$I = - \sum_{\mathbf{a}} P(\mathbf{a}) \log_2 P(\mathbf{a}), \quad (3)$$

where the sum is over all possible activity patterns \mathbf{a} . Note that $P(\mathbf{a}) = \int d\mathbf{c} P(\mathbf{a}|\mathbf{c}) P_{\text{env}}(\mathbf{c})$, where $P(\mathbf{a}|\mathbf{c})$ describes the mapping from \mathbf{c} to \mathbf{a} . Consequently, I depends on S_{ni} and the odor environment $P_{\text{env}}(\mathbf{c})$. In fact, I is maximized by sensitivities S_{ni} that are tailored to $P_{\text{env}}(\mathbf{c})$ such that all activity patterns \mathbf{a} are equally likely [12, 25].

The mutual information I can be approximated [26] in terms of the mean activities $\langle a_n \rangle$ and the covariance between receptors, $\text{cov}(a_n, a_m) = \langle a_n a_m \rangle - \langle a_n \rangle \langle a_m \rangle$, encoded by $P(\mathbf{a})$,

$$I \approx - \sum_n [\langle a_n \rangle \log_2 \langle a_n \rangle + (1 - \langle a_n \rangle) \log_2 (1 - \langle a_n \rangle)] - \frac{8}{\ln 2} \sum_{n < m} \text{cov}(a_n, a_m)^2, \quad (4)$$

which is an expansion up to quadratic order in $\text{cov}(a_n, a_m)$. The first term gives the information gained through each receptor in isolation. The second term describes the reduction of information due to correlations between different receptors. For both Eqs. 3 and 4, the maximal mutual information of N_r bits can only be obtained if

$$\langle a_n \rangle^* = \frac{1}{2} \quad \text{cov}(a_n, a_m)^* = 0. \quad (5)$$

Consequently, in a receptor array optimized for its natural environment, each receptor responds to about half of all odors and any pair of receptors is uncorrelated in its response to odors, assuming odors are presented with frequency $P_{\text{env}}(\mathbf{c})$.

These design principles follow from very general considerations, but they may not always be simultaneously achievable. To understand such constraints, we study how microscopic properties of receptor arrays (the sensitivities S_{ni}) determine both $\langle a_n \rangle$ and $\text{cov}(a_n, a_m)$. The mean receptor activity $\langle a_n \rangle$ is given by the probability that the associated excitation e_n exceeds 1, $\langle a_n \rangle = 1 - F_n(1)$, where $F_n(e_n)$ denotes the cumulative distribution function of e_n , see SI. The covariance $\text{cov}(a_n, a_m)$ can be estimated in terms of $\text{cov}_c(e_n, e_m)$ using a normal approximation around the maximum of I ,

see SI. These statistics of e_n can be calculated from Eq. 1 and read

$$\langle e_n \rangle_c = \sum_i S_{ni} \langle c_i \rangle \quad (6a)$$

$$\text{cov}_c(e_n, e_m) = \sum_{i,j} S_{ni} S_{mj} \text{cov}(c_i, c_j), \quad (6b)$$

where $\langle c_i \rangle$ and $\text{cov}(c_i, c_j)$ follow from $P_{\text{env}}(\mathbf{c})$. Combining Eqs. 4 and 6 to estimate mutual information, we can quantify how well an array's sensitivities S_{ni} are matched to natural odor statistics $P_{\text{env}}(\mathbf{c})$. As a computational matter, these equations also allow a rapid calculation of mutual information without calculating the full distribution $P(\mathbf{a})$.

B. Random sensitivity matrices

We next study which sensitivity matrices S_{ni} obey the optimization goals given in Eq. 5 for given odor statistics. Here, we will show that random S_{ni} with independent and identically distributed entries drawn from the right distribution can be close to optimal. This is because such matrices generically have low correlations and the resulting activities a_n are thus only weakly correlated. In the following, we study what distributions lead to $\langle a_n \rangle = \frac{1}{2}$ and under what conditions these matrices minimize $\text{cov}(a_n, a_m)$ for two different classes of odor distributions.

a. Narrow concentration distributions We begin with the simple case where the concentration distributions are narrow, $\sigma_i \ll \mu_i$. In this case, we can focus on determining which ligands appear in a mixture. Receptors that are optimal for this task must be highly sensitive to some ligands while they ignore the others, but the exact value of the sensitivity does not matter. This property can be encoded in a binary sensitivity matrix \hat{S}_{ni} where $\hat{S}_{ni} = 1$ if receptor n reacts to ligand i and $\hat{S}_{ni} = 0$ if it does not. We can then calculate activity statistics using Eqs. 2 and 6, as shown in the SI. In the simple case of uncorrelated mixtures ($p_{ij} = 0$ for $i \neq j$) $\langle a_n \rangle \approx \sum_i \hat{S}_{ni} p_i$ and $\text{cov}(a_n, a_m) \approx \sum_i \hat{S}_{ni} \hat{S}_{mi} p_i$. In the SI, we also calculate corrections due to the correlated appearance of ligands ($p_{ij} \neq 0$); e.g., $\langle a_n \rangle \approx \langle a_n \rangle_0 + \frac{1}{2}(1 - \langle a_n \rangle_0) \sum_{i,j} (\hat{S}_{ni} + \hat{S}_{nj} - \hat{S}_{ni} \hat{S}_{nj}) p_{ij}$, where $\langle a_n \rangle_0 = \sum_i \hat{S}_{ni} p_i$ is the receptor activity in the uncorrelated case.

In the case of uncorrelated mixtures, we find using Eq. 5 that \hat{S}_{ni} for optimal receptor arrays must satisfy

$$\sum_i \hat{S}_{ni}^* p_i = \frac{1}{2} \quad \sum_i \hat{S}_{ni}^* \hat{S}_{mi}^* p_i = 0. \quad (7)$$

Receptors are thus optimal if (i) the occurrence probabilities p_i of the ligands they react to add up to $\frac{1}{2}$ and (ii) no ligand activates multiple receptors. Since any given

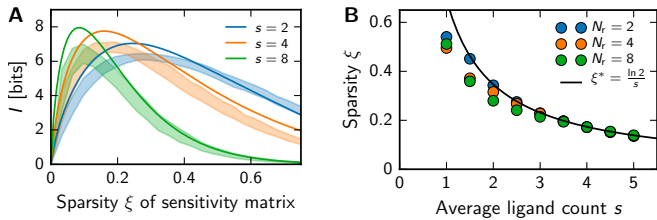


FIG. 2: Receptor arrays with random sensitivity matrices whose sparsity ξ is tuned to match natural statistics achieve near-optimal information transmission of odor composition. (A) Information I gained by $N_r = 8$ receptor as a function of the average sparsity ξ of random binary sensitivity matrices for mixtures made of s ligands drawn from a total of $N_l = 32$ ligands. Numerical results (shaded areas; mean \pm standard deviation; 32 samples) and analytical results (lines) following from Eq. 4 are shown. (B) Sparsity ξ of general binary sensitivity matrices that were numerically optimized for maximal I (symbols) is compared to the prediction from random binary matrices (solid line, Eq. S16) for different s and N_r at $N_l = 128$.

ligand is rare in natural odors, $p_i \ll \frac{1}{2}$, such optimization is equivalent to a partition problem where the N_l probabilities $\{p_i\}$ have to be put into N_r groups (i.e., a group of ligands for each receptor), such that the sum of the elements is close to $\frac{1}{2}$, while a minimal number of elements should appear in several groups. Eq. 4 gives the relative cost of violating these two possibly conflicting requirements.

This partition problem can be solved approximately using random binary sensitivity matrices. The ensemble of such matrices is characterized by a single parameter, the fraction of non-zero entries or sparsity ξ . Fig. 2A shows that there is an optimal sparsity ξ^* , at which I is maximized. It follows from $\langle a_n \rangle = \frac{1}{2}$ that

$$\xi^* \approx \frac{\ln 2}{s}, \quad (8)$$

where $s = \sum_i p_i$ is the mean mixture size, see SI. This condition for random matrices agrees well with the sparsity found from numerical optimization over all binary matrices, see Fig. 2B. However, for small s the sparsity ξ^* becomes large, which leads to significant correlations $\text{cov}(a_n, a_m)$ and thus reduced performance. Optimal matrices thus have a sparsity that is lower than predicted by Eq. S16 for small mixture sizes s , see Fig. 2B.

b. Wide concentration distributions In reality, odor concentration vary widely and receptor arrays must thus measure both odor composition and concentrations. The concentration of a single ligand can be measured if many receptors react to it with different sensitivities [7]. The receptor array is optimal for this task if all possible outputs occur with equal frequency. This is the case if the inverse of the sensitivities follows the same distribution as the ligand concentrations [12], which is known as Laughlin's principle. However, it is not clear how this principle can be generalized for measuring the concentration of multiple ligands simultaneously.

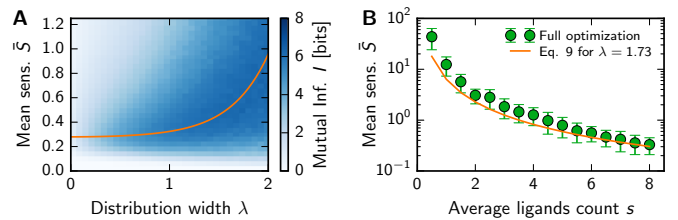


FIG. 3: Random receptor arrays with a suitable mean sensitivity \bar{S} and distribution width λ can transmit information about both odor concentration and composition. (A) I for log-normally distributed sensitivities as a function of the mean \bar{S} and width λ of the distribution for $N_r = 8$, $N_l = 16$, $p_i = \frac{1}{4}$, and $\mu_i = \sigma_i = 1$. The shown mean of I was calculated from Eqs. 1–3 using Monte-Carlo sampling of 32 realizations per point. The orange line marks the optimum given by Eq. 9. (B) Mean sensitivity \bar{S} for different s at $N_r = 8$, $N_l = 16$, and $\mu_i = \sigma_i = 1$. Numerical optimizations over general sensitivity matrices (symbols; mean \pm standard deviation; 64 samples) are compared to log-normally distributed matrices (solid line, Eq. 9) with $\lambda = 1.73$, equal to the mean of the numerical data.

We study this problem by considering random sensitivities that are log-normally distributed. This choice is motivated by the complex interaction between receptors and ligands, which typically leads to normally distributed binding energies [27]. We will show later that experimentally measured sensitivities indeed appear to be log-normally distributed. Log-normal distributions are characterized by two parameters, the mean \bar{S} and the standard deviation λ of the underlying normal distribution. We thus next ask how these parameters have to be chosen to maximize the mutual information I . To estimate I , we need to consider the excitations e_n , which approximately also follow a log-normal distribution [28]. Their statistics are given by Eq. 6 and read $\langle e_n \rangle_{c,S} = \bar{S} \langle c_{\text{tot}} \rangle$ and $\text{cov}_{c,S}(e_n, e_m) = \bar{S}^2 \text{var}(c_{\text{tot}}) + \delta_{nm} \text{var}(S) \sum_i \langle c_i^2 \rangle$, where $c_{\text{tot}} = \sum_i c_i$ and $\text{var}(S) = \bar{S}^2 [\exp(\lambda^2) - 1]$. We use this to calculate $\langle a_n \rangle$ from Eq. 2 and find that the receptor array is optimal ($\langle a_n \rangle = \frac{1}{2}$) if

$$\bar{S} = \frac{1}{\langle c_{\text{tot}} \rangle} \left[1 + \frac{\text{var}(c_{\text{tot}})}{\langle c_{\text{tot}} \rangle^2} + \frac{\sum_i \langle c_i^2 \rangle}{\langle c_{\text{tot}} \rangle^2} (e^{\lambda^2} - 1) \right]^{\frac{1}{2}}, \quad (9)$$

see SI. We test this equation by numerically calculating the mutual information I as a function of \bar{S} and λ . Fig. 3A shows that Eq. 9 predicts the optimal parameters of log-normally distributed sensitivities very well. Fig. 3B shows that this result also predicts the mean \bar{S} for numerical optimizations over general sensitivity matrices.

Log-normally distributed sensitivities perform badly if the distribution width λ is small, see Fig. 3A. This is expected since receptors with narrowly distributed S_{ni} respond similarly to all ligands, leading to large correlations $\text{cov}(a_n, a_m)$ and thus reduced performance I . Interestingly, for large enough λ the correlations are so small that the exact value of λ does not influence I signifi-

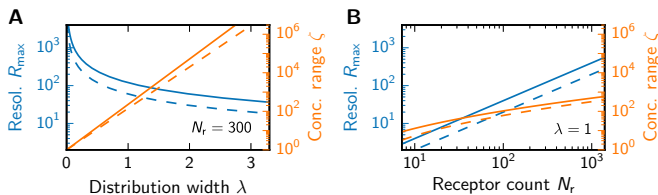


FIG. 4: The width λ of the sensitivity distribution has opposing effects on concentration resolution R_{\max} (blue, Eq. 10) and range ζ (orange, Eq. 11). (A) R_{\max} and ζ as a function of the width λ for $N_r = 300$. (B) R_{\max} and ζ as a function of N_r for $\lambda = 1$. Shown are $\eta = 1$ (solid lines) and $\eta = 2$ (dashed lines).

cantly, see Fig. 3A. In fact, for very large λ , the S_{ni} are likely very large or very small compared to \bar{S} . When \bar{S} is chosen according to Eq. 9, receptors can thus only detect whether ligands are present or not, corresponding to the binary sensitivities discussed above, which cannot resolve the concentration of the ligands. Consequently, λ must influence how well such receptor arrays can resolve concentrations.

c. Trade-off between concentration resolution and mixture discriminability When the distribution width λ is large, the receptor arrays have similar performance I , so they are equally good at the combined problem of resolving concentrations and discriminating mixtures. However, the performance in the individual problems can vary widely. Since in many contexts we might wish to trade off performance, say, by sacrificing some ability to discriminate mixtures in favor of a better concentration resolution, we next investigate these properties in detail.

We define the concentration resolution R as the ratio of the concentration c at which a single ligand is presented and the concentration change δc that is necessary to register a change, $R = c/\delta c$. Here, we consider the simple case where η additional receptors have to be excited to register a change in concentration. R is a function of the concentration c at which it is measured and its maximal value

$$R_{\max} = \frac{N_r}{\sqrt{2\pi\eta}\lambda} \quad (10)$$

is obtained for $c = \bar{S}^{-1} \exp(\frac{1}{2}\lambda^2)$, which is the inverse of the median of the sensitivity distribution, see SI.

The range of concentrations that can be detected by the receptor array is given by the ratio of the largest concentration c_{\max} at which concentration differences can be detected to the lowest detectable concentration c_{\min} , the odor detection threshold [29]. In terms of η , the logarithm of the concentration range $\zeta = c_{\max}/c_{\min}$ reads (see SI)

$$\ln(\zeta) = 2\sqrt{2}\lambda \operatorname{erf}^{-1}\left(1 - \frac{2\eta}{N_r}\right), \quad (11)$$

where $\operatorname{erf}^{-1}(z)$ is the inverse error function. Eq. 11 shows that λ determines the number of concentration decades over which the receptor array is sensitive.

Taken together, λ has opposing effects on the resolution and the range of concentration measurements, see Fig. 4A. Consequently, λ can be tuned either for receptors that resolve concentrations well or cover a large concentration range. If only single ligands are measured, the optimal λ only depends on the concentration distribution $P_{\text{env}}(c)$. In this case, the mutual information I can be calculated from the resolution function $R(c)$ and optimizing $R(c)$ is equivalent to maximizing I [30]. For odor mixtures, I accounts for a combination of the concentration resolution and the mixture discrimination and maximizing I does not uniquely determine an optimal receptor array. We thus next study how the distribution width λ influences the ability to discriminate mixtures.

We first consider mixtures of s ligands, each at concentration c , and determine the maximal size s_{\max} where adding an additional ligand does not significantly alter the activity pattern. s_{\max} is given by the largest s that obeys (see SI)

$$\frac{d\langle a_n \rangle_S}{ds} \geq \frac{\eta}{N_r}, \quad (12)$$

where $\langle a_n \rangle_S \approx 1 - F_{\text{LN}}(c^{-1}; \bar{S}s, \text{var}(S)s)$ with $F_{\text{LN}}(x; \mu, \sigma^2)$ being the cumulative distribution function of a log-normal distribution with mean μ and variance σ^2 . Fig. 5A shows that s_{\max} increases with decreasing concentrations, but if the concentration falls below the odor detection threshold, individual ligands cannot be detected (dotted lines).

Not all mixtures with less than s_{\max} ligands can be distinguished from each other. We show this by calculating the Hamming distance h of the activity patterns \mathbf{a} of two mixtures, i.e., the number of differences in the output. For simplicity, we consider mixtures that contain s ligands, sharing s_b of them. In this case, a given receptor is activated by one of the mixtures if $e_b + e_d > 1$, where e_b and e_d are the excitations caused by the s_b shared and the $s - s_b$ different ligands, respectively. Approximating the probability distribution of the excitations as a log-normal distribution, we can calculate the expected distance h , see SI. Fig. 5B shows that this approximation (solid lines) agrees well with numerical calculations (symbols). The figure also shows that mixtures can only be distinguished well if the concentration of the constituents is in the right range. This is because receptors are barely excited for too small concentrations while they are saturated for large concentrations. The distance h also strongly depends on the number s_b of shared ligands between the two mixtures, which has also been shown experimentally [31]. The distance vanishes for $s_b = s$, but Fig. 5B shows that a single different ligand can be sufficient to distinguish mixtures in the right concentration range (green line). This range increases with the width λ of the sensitivity distribution, similar to the range over which concentrations can be measured, see Eq. 11.

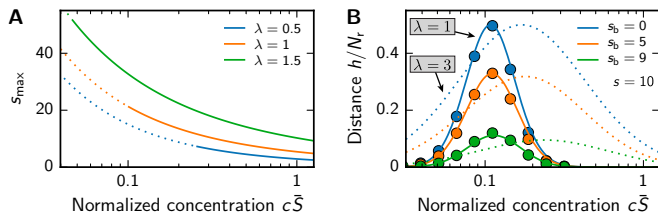


FIG. 5: The discriminability of mixtures strongly depends on the concentrations at which odors are presented. (A) Maximal mixture size s_{\max} (from Eq. 12) as a function of the ligand concentration c for different widths λ of the sensitivity distribution at $N_r/\eta = 300$. Dotted lines indicate where c is below the detection threshold for single ligands. (B) Mean difference h in the activation pattern of two mixtures of size $s = 10$ as a function of c for different numbers s_b of shared ligands and widths λ . Analytical results (lines) are compared to numerical simulations (symbols).

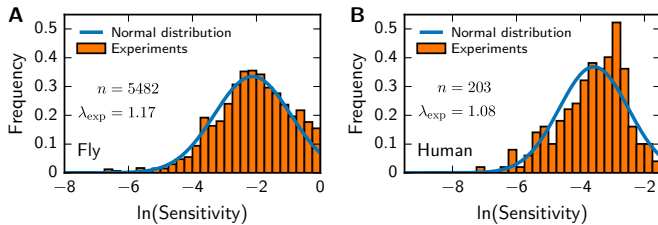


FIG. 6: Sensitivities of olfactory receptors appear to be log-normally distributed for (A) flies [32] and (B) humans [33]. The histograms of the logarithms of n entries of the sensitivity matrix (orange) are compared to a normal distribution (blue) with the same mean and standard deviation λ_{exp} .

C. Experimentally measured receptor arrays

The response of receptors to individual ligands has been measured experimentally for flies [32] and humans [33]. We use these published data to estimate the statistics of realistic sensitivity matrices as described in the SI. Fig. 6 shows the histograms of the logarithms of the sensitivities for flies and humans. Both histograms are close to a normal distribution, with similar standard deviations $\lambda_{\text{exp}} \approx 1.1$, which implies log-normally distributed sensitivities. Using a simple binding model between receptors and ligands, λ_{exp} can also be interpreted as the standard deviation of the interaction energies, see SI. Consequently, these interaction energies exhibit a similar variation on the order of one $k_B T$ for both organisms, which could be caused by the biophysical similarity of the receptors.

We next use the measured log-normal distribution for the sensitivities to compare the concentration resolution R predicted by Eq. 10 to measured ‘just noticeable relative differences’ R^{-1} [22]. For humans ($N_r = 300$), the measured values are as low as 4% [34], which implies $\eta\lambda \approx 4.8$. Using $\lambda \approx 1.1$, this suggests that about 4 receptors have to be activated until a change in concentration can be registered. Additionally, our theory predicts that

humans can sense concentrations over about 2.6 orders of magnitude, which follows from Eq. 11 for $\lambda = 1.1$, $\eta = 1$, and $N_r = 300$. However, we are not aware of any measurements of the concentration range for humans.

Our theory also predicts the maximal number of ligands that can be distinguished as a function of the concentration c of the individual ligands. For $\lambda \approx 1.1$, we expect that the maximal number s_{\max} of ligands in a mixture is around 20 if individual ligands can be detected, see Fig. 5A. Experimental studies report similar values, e.g., $s_{\max} \approx 15$ [35] and $s_{\max} < 30$ [6]. However, Fig. 5A shows that s_{\max} strongly depends on the concentration of the individual ligands and thus on experimental details. Similarly, how well mixtures can be discriminated also depends strongly on the ligand concentration. Fig. 5B shows that the concentration range over which mixtures can be distinguished is less than an order of magnitude for $\lambda \approx 1.1$.

II. DISCUSSION

We studied how arrays of olfactory receptors can be used to measure odor mixtures, focusing on the combinatorial code of olfaction, i.e., how the combined response of multiple receptors can encode the composition (quality) and the concentration (quantity) of odors. Such arrays are optimal if each receptor responds to about half of the encountered odors and the receptors have distinct ligand binding profiles to minimize correlations.

Our simple model of binary receptors can in principle distinguish a huge number of odors, since there are $\sim 10^{90}$ different output combinations for $N_r = 300$. However, it is not clear whether all outputs are achievable and how they are used to distinguish odors. We showed that the mean receptor sensitivity must be tailored to the mean concentration to best use the large output space. Another important parameter of receptor arrays is the fraction of receptors that is activated by a single ligand, which is equivalent to the sparsity ξ in the simple case of binary sensitivities. If ξ is small, combining different ligands typically leads to unique output patterns that allow to identify the mixtures, but the concentration of isolated ligands cannot be measured reliably, since only few receptors are involved. Conversely, if ξ is large, mixtures of multiple ligands will excite almost all receptors, such that neither the odor quality nor the odor quantity can be measured reliably. However, here, the concentration of an isolated ligand can be measured precisely. We discussed this property in detail for sensitivities that are log-normally distributed, where the width λ controls whether mixtures can be distinguished well or concentrations can be measured reliably. Interestingly, experiments find that individual ligands at moderate concentration only excite few glomeruli [36], but natural odors at native concentrations can excite many [37]. This could imply that the sensitivities are indeed adapted such that each receptor is excited about half the times for natural

odors.

Our model implies that having more receptor types can improve all properties of the receptor array. In particular, both the concentration resolution R and the typical distance h between mixtures are proportional to N_r , a prediction that can be tested experimentally. For instance, mice, with $N_r \approx 1000$ receptor types, are very good at identifying a single odor in a mixture [38], but flies, with $N_r = 52$ [32], should perform much worse. However, quantitative comparisons might be difficult since the discrimination performance strongly depends on the normalized concentration $c\bar{S}$ at which odors are presented. In fact, we predict that mixtures can hardly be distinguished if the concentration of the individual ligands is changed by an order of magnitude, see Fig. 5B.

Our results also apply to artificial chemical sensor arrays known as 'artificial noses' [39, 40]. Having more sensors improves the general performance of the array, but it is also important to tune the sensitivity of individual sensors. Here, sensors should be as diverse as possible while still responding to about half the incoming mixtures. Unfortunately, building such chemical sensors is difficult and their binding properties are hard to control [40]. If the sensitivity matrix of the sensor array is known, our theory can be used to estimate the information I_n that receptor n contributes as $I_n \approx H_b(\langle a_n \rangle) - \frac{4}{\ln 2} \sum_{m \neq n} \text{cov}(a_n, a_m)^2$ where $H_b(p) = -p \log_2 p - (1-p) \log_2 (1-p)$, such that $I = \sum_n I_n$, see Eq. 4. This can then be used for identifying poor receptors that contribute only little information to the overall results.

Our focus on the combinatorial code of the olfactory system certainly neglects intricate details of the system. For instance, we consider sensitivity matrices with independent entries, but biophysical constraints will

cause chemically similar ligands to excite similar receptors [8, 41]. This is important because it makes it difficult to distinguish similar ligands [42] and it might thus be worthwhile to dedicate more receptors to such a part of chemical space. Additionally, receptors or glomeruli might interact with each other, e.g., causing inhibition reducing the signal upon binding a ligand [43]. We can in principle discuss inhibition in our model by allowing for negative sensitivities, but more complicated features cannot be captured by the linear relationship in Eq. 1. One important non-linearity is the dose-response curve of individual receptor neurons [20], which we approximate by a step function, see Eq. 2. This simplification reduces the information capacity of a single glomerulus to 1 bit, while it is likely higher in reality. However, we expect that allowing for multiple output levels would only increase the concentration resolution and not change the discriminability of mixtures very much [22]. It would be interesting to see how such an extended model can measure heterogeneous mixtures with ligands at different concentrations.

Acknowledgments

We thank Michael Tikhonov and Carl Goodrich for helpful discussions and a critical reading of the manuscript. This research was funded by the National Science Foundation through DMR-1435964, the Harvard Materials Research Science and Engineering Center DMR-1420570, the Division of Mathematical Sciences DMS-1411694, and the German Science Foundation through ZW 222/1-1. MPB is an investigator of the Simons Foundation.

-
- [1] Kazushige Touhara and Leslie B Vosshall. Sensing odorants and pheromones with chemosensory receptors. *Annu Rev Physiol*, 71:307–32, 2009.
 - [2] Chih-Ying Su, Karen Menuz, and John R Carlson. Olfactory perception: receptors, cells, and circuits. *Cell*, 139(1):45–59, Oct 2009.
 - [3] Joel D Mainland, Johan N Lundström, Johannes Reisert, and Graeme Lowe. From molecule to mind: an integrative perspective on odor intensity. *Trends Neurosci.*, 37(8):443–454, 2014.
 - [4] Christophe Verbeurgt, Françoise Wilkin, Maxime Tarabichi, Françoise Gregoire, Jacques E Dumont, and Pierre Chatelain. Profiling of olfactory receptor gene expression in whole human olfactory mucosa. *PLOS ONE*, 9(5):e96333, 2014.
 - [5] Mathias Dunkel, Ulrike Schmidt, Swantje Struck, Lena Berger, Bjoern Gruening, Julia Hossbach, Ines S Jaeger, Uta Effmert, Birgit Piechulla, Roger Eriksson, Jette Knudsen, and Robert Preissner. Superscent—a database of flavors and scents. *Nucleic Acids Res*, 37(Database issue):D291–4, Jan 2009.
 - [6] Tali Weiss, Kobi Snitz, Adi Yablonka, Rehan M Khan, Danyel Gafso, Elad Schneidman, and Noam Sobel. Perceptual convergence of multi-component mixtures in olfaction implies an olfactory white. *Proc. Natl. Acad. Sci. USA*, 109(49):19959–19964, 2012.
 - [7] JJ Hopfield. Odor space and olfactory processing: collective algorithms and neural implementation. *Proc. Natl. Acad. Sci. USA*, 96(22):12506–12511, 1999.
 - [8] Bettina Malnic, Junzo Hirono, Takaaki Sato, and Linda B Buck. Combinatorial receptor codes for odors. *Cell*, 96(5):713–723, 1999.
 - [9] Yehudit Hasin, Tsviya Olender, Miriam Khen, Claudia Gonzaga-Jauregui, Philip M Kim, Alexander Eckehart Urban, Michael Snyder, Mark B Gerstein, Doron Lancet, and Jan O Korb. High-resolution copy-number variation map reflects human olfactory receptor diversity and evolution. *PLoS Genet*, 4(11):e1000249, Nov 2008.
 - [10] Alison Maresh, Diego Rodriguez Gil, Mary C Whitman, and Charles A Greer. Principles of glomerular organization in the human olfactory bulb—implications for odor processing. *PLOS ONE*, 3(7):e2640, 2008.
 - [11] Michael Leon and Brett A Johnson. Olfactory coding in the mammalian olfactory bulb. *Brain Res. Rev.*,

- 42(1):23–32, 2003.
- [12] S Laughlin. A simple coding procedure enhances a neuron’s information capacity. *Z Naturforsch C*, 36(9-10):910–2, 1981.
- [13] Ruderman and Bialek. Statistics of natural images: Scaling in the woods. *Phys. Rev. Lett.*, 73(6):814–817, Aug 1994.
- [14] Michael S Lewicki. Efficient coding of natural sounds. *Nat Neurosci*, 5(4):356–63, Apr 2002.
- [15] Gasper Tkacik, Curtis G Callan, Jr, and William Bialek. Information flow and optimization in transcriptional regulation. *Proc. Natl. Acad. Sci. USA*, 105(34):12265–70, Aug 2008.
- [16] Robert Hummel. Image enhancement by histogram transformation. *Comput. Gr. Image Process.*, 6(2):184–195, 1977.
- [17] Geraldine A Wright and Mitchell GA Thomson. Odor perception and the variability in natural odor scenes. In J. Romeo, editor, *Integrative Plant Biochemistry*, volume 39 of *Recent Advances in Phytochemistry*, chapter 8, pages 191–226. Elsevier, 2005.
- [18] John P McGann, Nicolás Pérez, Melanie A Gainey, Christina Muratore, Adam S Elias, and Matt Wachowiak. Odorant representations are modulated by intra- but not interglomerular presynaptic inhibition of olfactory sensory neurons. *Neuron*, 48(6):1039–53, Dec 2005.
- [19] Da Yu Lin, Stephen D Shea, and Lawrence C Katz. Representation of natural stimuli in the rodent main olfactory bulb. *Neuron*, 50(6):937–949, 2006.
- [20] Johannes Reiser and Diego Restrepo. Molecular tuning of odorant receptors and its implication for odor signal processing. *Chemical senses*, 34:535–545, 2009.
- [21] G Lowe and G H Gold. Olfactory transduction is intrinsically noisy. *Proc. Natl. Acad. Sci. USA*, 92(17):7864–8, Aug 1995.
- [22] Alexei Koulakov, Alan Gelperin, and Dmitry Rinberg. Olfactory coding with all-or-nothing glomeruli. *J. Neurophysiol.*, 98(6):3134–3142, 2007.
- [23] Charles F Stevens. What the fly’s nose tells the fly’s brain. *Proc. Natl. Acad. Sci. USA*, 112(30):9460–5, Jul 2015.
- [24] Jette T Knudsen, Lars Tollsten, and L Gunnar Bergström. Floral scents checklist of volatile compounds isolated by head-space techniques. *Phytochemistry*, 33(2):253–280, 1993.
- [25] Joseph J Atick. Could information theory provide an ecological theory of sensory processing? *Network*, 3(2):213–251, 1992.
- [26] Vitor Sessak and Rémi Monasson. Small-correlation expansions for the inverse ising problem. *J. Phys. A*, 42(5):055001, 2009.
- [27] Doron Lancet, Ella Sadovsky, and Eyal Seidemann. Probability model for molecular recognition in biological receptor repertoires: significance to the olfactory system. *Proc. Natl. Acad. Sci. USA*, 90(8):3715–3719, 1993.
- [28] Lawrence F Fenton. The sum of log-normal probability distributions in scatter transmission systems. *Communications Systems, IRE Transactions on*, 8(1):57–67, 1960.
- [29] Michael H Abraham, Ricardo Sánchez-Moreno, J Enrique Cometto-Muñiz, and William S Cain. An algorithm for 353 odor detection thresholds in humans. *Chemical senses*, page bjr094, 2011.
- [30] William Bialek. *Biophysics: Searching for Principles*. Princeton University Press, 2012.
- [31] C Bushdid, MO Magnasco, LB Vosshall, and A Keller. Humans can discriminate more than 1 trillion olfactory stimuli. *Science*, 343(6177):1370–1372, 2014.
- [32] Daniel Münch and C Giovanni Galizia. DoOR 2.0-comprehensive mapping of *Drosophila melanogaster* odorant responses. *bioRxiv*, page 027920, 2015.
- [33] Joel D Mainland, Yun R Li, Ting Zhou, Wen Ling L Liu, and Hiroaki Matsunami. Human olfactory receptor responses to odorants. *Sci Data*, 2:150002, 2015.
- [34] William S Cain. Differential sensitivity for smell: ”noise” at the nose. *Science*, 195(4280):796–798, 1977.
- [35] A Jinks and D G Laing. A limit in the processing of components in odour mixtures. *Perception*, 28(3):395–404, 1999.
- [36] Harumi Saito, Qiuyi Chi, Hanyi Zhuang, Hiro Matsunami, and Joel D Mainland. Odor coding by a mammalian receptor repertoire. *Science signaling*, 2(60):ra9, 2009.
- [37] Roberto Vincis, Olivier Gschwend, Khaleel Bhaukaurally, Jonathan Beroud, and Alan Carleton. Dense representation of natural odorants in the mouse olfactory bulb. *Nat. Neurosci.*, 15(4):537–539, 2012.
- [38] Dan Rokni, Vivian Hemmelder, Vikrant Kapoor, and Venkatesh N Murthy. An olfactory cocktail party: figure-ground segregation of odorants in rodents. *Nat. Neurosci.*, 17(9):1225–32, Sep 2014.
- [39] K J Albert, N S Lewis, C L Schauer, G A Sotzing, S E Stitzel, T P Vaid, and D R Walt. Cross-reactive chemical sensor arrays. *Chem Rev*, 100(7):2595–626, Jul 2000.
- [40] Shannon E Stitzel, Matthew J Aernecke, and David R Walt. Artificial noses. *Annu. Rev. Biomed. Eng.*, 13:1–25, 2011.
- [41] Elissa A Hallem and John R Carlson. Coding of odors by a receptor repertoire. *Cell*, 125(1):143–160, 2006.
- [42] Margot Perez, Martin Giurfa, and Patrizia d’Ettorre. The scent of mixtures: rules of odour processing in ants. *Scientific Reports*, 5, 2015.
- [43] Kirill Ukhanov, Elizabeth A Corey, Daniela Brunert, Katharina Klasen, and Barry W Ache. Inhibitory odorant signaling in mammalian olfactory receptor neurons. *J Neurophysiol*, 103(2):1114–22, Feb 2010.
- [44] Nikolaus Hansen. The CMA evolution strategy: a comparing review. In *Towards a new evolutionary computation*, pages 75–102. Springer, 2006.
-

Supplemental Information: Receptor arrays optimized for natural odor statistics

S1. RECEPTOR SENSITIVITIES

A. Equilibrium binding model

We consider a simple model where receptors R_n get activated when they bind ligands L_i . This binding is described by the chemical reaction $R_n + L_i \rightleftharpoons R_n L_i$, where $R_n L_i$ is the receptor-ligands complex. The equilibrium of the reaction is characterized by a binding constant K_{ni} , which reads

$$K_{ni} = \exp\left(\frac{E_{ni}}{k_B T}\right), \quad (\text{S1})$$

where E_{ni} is the interaction energy between receptor n and ligand i . In equilibrium, the concentrations denoted by square brackets obey $[R_n L_i] = K_{ni} \cdot [R_n][L_i]$. Hence,

$$[R_n L_i] = \frac{c_n^{\text{rec}} K_{ni} c_i}{1 + \sum_i K_{ni} c_i}, \quad (\text{S2})$$

where we consider the case where multiple ligands compete for the same receptor. Here, $c_n^{\text{rec}} = [R_n] + \sum_i [R_n L_i]$ denotes the fixed concentration of receptors and $c_i = [L_i]$ is the concentration of free ligands. We consider a simple receptor model in which the excitation e_n^{rec} of a receptors of type n is proportional to the concentration of bound ligands,

$$e_n^{\text{rec}} = \alpha_n \sum_i [R_n L_i], \quad (\text{S3})$$

where α_n characterizes the excitability of receptor type n . As discussed in the main text, the excitations of all receptors of a given type are accumulated in the respective glomeruli, whose excitation e_n^{glo} is thus given by $e_n^{\text{glo}} = N_n^{\text{rec}} e_n^{\text{rec}}$, where N_n^{rec} is the number of receptors of type n . In the simple case of binary outputs, a glomerulus becomes active if its excitation exceeds a threshold t_n , $a_n = \Theta(e_n^{\text{glo}} - t_n)$, where $\Theta(z)$ denotes the Heaviside step function. We consider the case $\alpha_n c_n^{\text{rec}} \gg t_n$, where the glomerulus signals before the associated receptors become saturated. In this case, we can linearize Eq. S2 and introduce the rescaled quantities

$$e_n = \frac{e_n^{\text{glo}}}{t_n} \quad \text{and} \quad S_{ni} = \frac{\alpha_n N_n^{\text{rec}} c_n^{\text{rec}}}{t_n} K_{ni} \quad (\text{S4})$$

to obtain Eqs. 1–2 of the main text.

A simple theory [27] predicts that the interaction energies E_{ni} between receptors and ligands are normal distributed. For the receptor model described above, this implies log-normal distributed binding constant K_{ni} , see Eq. S1. In this case, the sensitivities S_{ni} will also be log-normal distributed, see Eq. S4.

B. Measured receptor sensitivities

Response matrices have been measured experimentally for flies [32] and humans [33]. The fly database has been constructed by merging data from many studies that used various methods to measure receptor responses [32]. It contains a non-zero response for 5482 receptor-ligand pairs, covering all 52 receptors that are present in flies. Fig. 6A in the main text shows the histogram of the logarithm of the associated sensitivities together with a normal distribution with the same mean and variance as the data.

The only comprehensive study of human olfactory receptors used a luciferase assay to measure receptor responses *in vitro* [33]. They report the intensity of clones of 511 human olfactory receptors in response to various concentrations of 73 ligands. Typically, the intensity of a given receptor-ligand pair is monotonously increasing as a function of ligand concentration c . We normalize the intensity to lie between 0 and 1 and fit a hyperbolic tangent function to determine the concentration c_* at which the normalized intensity reaches 0.5. Here, the only fit parameters are the concentration c_* and the slope of the tangent function at this point. We exclude poor fits, where the relative error in either parameters is above 50%. This leaves us with 203 of the 623 receptor-ligand combinations, for which we then define the sensitivity as c_*^{-1} . Fig. 6B in the main text shows the histogram of these sensitivities together with a normal distribution with the same mean and variance as the data.

S2. RECEPTOR RESPONSE

We next discuss the statistics of receptor response as a function of the odor statistics $P_{\text{env}}(\mathbf{c})$. We first analyze binary mixtures, where ligands are either present or not, and then consider the more complex case of continuous mixtures, which require a distribution of sensitivities to be able to sense different concentrations.

A. Binary mixtures

We consider statistics of binary mixtures ($c_i \in \{0, 1\}$) that are given by

$$P_{\text{env}}(\mathbf{c}) = \frac{1}{Z_J[h]} \exp\left(\sum_{i,j} J_{ij} c_i c_j + \sum_i h_i c_i\right), \quad (\text{S5})$$

where h_i denotes the commonness of ligand i and J_{ij} parameterizes correlations between ligands i and j . Without loss of generality, J_{ij} is symmetric with zeros on the diagonal. The associated partition function Z_J , which

ensures that $\int d\mathbf{c} P_{\text{env}}(\mathbf{c}) = 1$, reads

$$Z_J[h] = \int d\mathbf{c} e^{J_{ij}c_i c_j + h_i c_i}, \quad (\text{S6})$$

where the integral is over all binary mixtures. Note that we here and below use the Einstein summation convention, i.e. we imply summation over repeated indices in a formula.

d. Uncorrelated binary mixtures For uncorrelated mixtures ($J_{ij} = 0$), the partition function reads $Z_0[h] = \int d\mathbf{c} e^{h_i c_i}$. The probability $p_i^* = \langle c_i \rangle_h$ of finding a ligand then reads

$$p_i^* = \frac{1}{Z_0[h]} \int d\mathbf{c} c_i e^{h_j c_j} = \frac{e^{h_i}}{1 + e^{h_i}}, \quad (\text{S7})$$

where the notation $\langle \cdot \rangle_h$ and the index $*$ denote the average with respect to uncorrelated mixtures. The covariance $p_{ij}^* = \langle c_i c_j \rangle_h - \langle c_i \rangle_h \langle c_j \rangle_h$ follows from

$$\langle c_i c_j \rangle_h = \frac{1}{Z_0[h]} \int d\mathbf{c} c_i c_j e^{h_k c_k} = p_i^* p_j^* - \delta_{ij} (p_i^*)^2 + \delta_{ij} p_i^* \quad (\text{S8})$$

and reads

$$p_{ij}^* = \delta_{ij} p_i^* (1 - p_i^*). \quad (\text{S9})$$

The receptor activity a_n , given by Eq. 2 in the main text, is a function of the excitation $e_n = S_{ni} c_i$. For binary mixtures, the step-function in Eq. 2 can be approximated by

$$a_n \approx 1 - e^{-\gamma e_n}, \quad (\text{S10})$$

which becomes exact in the limit $\gamma \rightarrow \infty$. We use this to calculate the moments of $\bar{a}_n = 1 - a_n$,

$$\langle \bar{a}_n \rangle_h = \frac{Z_0[h^{(n)}]}{Z_0[h]} \quad \langle \bar{a}_n \bar{a}_m \rangle_h = \frac{Z_0[h^{(nm)}]}{Z_0[h]}, \quad (\text{S11})$$

where

$$h_i^{(n)} = h_i - \gamma \hat{S}_{ni} \quad (\text{S12a})$$

$$h_i^{(nm)} = h_i - \gamma (\hat{S}_{ni} + \hat{S}_{mi}). \quad (\text{S12b})$$

In particular, we have in the limit $\gamma \rightarrow \infty$,

$$Z_0[h] = \prod_i (1 + e^{h_i}) \quad (\text{S13a})$$

$$Z_0[h^{(n)}] = \prod_i [1 + e^{h_i} (1 - \hat{S}_{ni})] \quad (\text{S13b})$$

$$Z_0[h^{(nm)}] = \prod_i [1 + e^{h_i} (1 - \hat{S}_{ni}) (1 - \hat{S}_{mi})]. \quad (\text{S13c})$$

Hence,

$$\langle a_n \rangle_h = 1 - \prod_i (1 - \hat{S}_{ni} p_i^*) \quad (\text{S14a})$$

$$\begin{aligned} \text{cov}_h(a_n, a_m) &= \prod_i [1 - (\hat{S}_{ni} + \hat{S}_{mi} - \hat{S}_{ni} \hat{S}_{mi}) p_i^*] \\ &\quad - \prod_i (1 - \hat{S}_{ni} p_i^*) (1 - \hat{S}_{mi} p_i^*). \end{aligned} \quad (\text{S14b})$$

We develop these equations to linear order in p_i^* to obtain Eqs. 7 of the main text.

The receptor activity for binary sensitivity matrices with independent and identically distributed entries is described by

$$\langle a_n \rangle_h = 1 - \prod_i (1 - \xi p_i^*) \approx \xi s, \quad (\text{S15a})$$

$$\text{cov}_h(a_n, a_m) \approx \xi^2 s, \quad (\text{S15b})$$

where $s = \sum_i \langle c_i \rangle_h$ is the mean number of ligands in a mixture. Here, ξ denotes the sparsity of \hat{S}_{ni} , which is the only parameter of the random ensemble. The optimal sparsity ξ^* at which I is maximized is given by the condition $\langle a_n \rangle_h = \frac{1}{2}$. Using Eq. S14a and solving for ξ , we obtain

$$\xi^* \approx N_1 \frac{1 - 2^{-\frac{1}{N_1}}}{s}, \quad (\text{S16})$$

which for large N_1 at constant s becomes $\xi^* = s^{-1} \ln 2$.

e. Correlated binary mixtures We consider weakly correlated mixtures, where we expand all results to linear order in J_{ij} . Hence,

$$Z_J[h] \approx Z_0[h] \cdot (1 + J_{ij} \langle c_i \rangle_h \langle c_j \rangle_h). \quad (\text{S17})$$

The probability $p_i = \langle c_i \rangle_J$ with which ligand i appears reads

$$\begin{aligned} p_i &= \frac{1}{Z_J[h]} \int d\mathbf{c} c_i e^{J_{jk} c_j c_k + h_j c_j} \\ &\approx \langle c_i \rangle_h [1 - J_{jk} \langle c_j \rangle_h \langle c_k \rangle_h] + J_{jk} \langle c_i c_j c_k \rangle_h, \end{aligned} \quad (\text{S18})$$

where

$$\begin{aligned} \langle c_i c_j c_k \rangle_h &= p_i^* p_j^* p_k^* + \delta_{ij} \bar{p}_i^* p_i^* p_k^* + \delta_{ik} p_i^* \bar{p}_i^* p_j^* \\ &\quad + \delta_{jk} p_i^* p_j^* \bar{p}_j^* + \delta_{ij} \delta_{jk} p_i^* p_i^* (1 - 2p_i^*) \end{aligned} \quad (\text{S19})$$

with $\bar{p}_i^* = 1 - p_i^*$. Hence,

$$p_i \approx p_i^* [1 + 2J_{ij} \bar{p}_i^* p_j^*], \quad (\text{S20})$$

where we used $J_{ij} = J_{ji}$ and $\text{diag}(J) = \mathbf{0}$. Similarly, the covariance $p_{ij} = \langle c_i c_j \rangle_J - \langle c_i \rangle_J \langle c_j \rangle_J$ between ligands can be calculated from $\langle c_i c_j \rangle_J$, which involves

$$\begin{aligned} J_{kl} \langle c_i c_j c_k c_l \rangle &= \delta_{ij} p_i^* \bar{p}_i^* [2J_{ki} p_k^* (1 - 2p_i^*) + J_{kl} p_l^* p_k^*] \\ &\quad + p_i^* p_j^* [2J_{ij} \bar{p}_i^* \bar{p}_j^* + 2J_{il} \bar{p}_i^* p_l^* + 2J_{jl} \bar{p}_j^* p_l^* + J_{kl} p_l^* p_k^*] \end{aligned} \quad (\text{S21})$$

and thus reads

$$\begin{aligned} \langle c_i c_j \rangle_J &\approx \langle c_i c_j \rangle_h [1 - J_{kl} \langle c_k \rangle_h \langle c_l \rangle_h] + J_{kl} \langle c_i c_j c_k c_l \rangle_h \\ &= p_i^* p_j^* [1 + 2J_{ij} \bar{p}_i^* \bar{p}_j^* + 2J_{il} \bar{p}_i^* p_l^* + 2J_{jl} \bar{p}_j^* p_l^*] \\ &\quad + \delta_{ij} p_i^* \bar{p}_i^* [1 + 2J_{il} p_l^* (1 - 2p_i^*)], \end{aligned} \quad (\text{S22})$$

where we used Eq. S8. Hence,

$$p_{ij} = \langle c_i c_j \rangle_J - \langle c_i \rangle_J \langle c_j \rangle_J \approx \delta_{ij} p_i \bar{p}_i + 2J_{ij} p_i^* \bar{p}_i^* p_j^*, \quad (\text{S23})$$

where $\bar{p}_i = 1 - p_i$. The statistics of the receptor activity $a_n = 1 - \bar{a}_n$ follow from

$$\langle \bar{a}_n \rangle_J = \frac{Z_J[h^{(n)}]}{Z_J[h]} \quad \langle \bar{a}_n \bar{a}_m \rangle_J = \frac{Z_J[h^{(nm)}]}{Z_J[h]} \quad (\text{S24})$$

and read

$$\langle \bar{a}_n \rangle_J \approx \langle \bar{a}_n \rangle_h \cdot \frac{1 + J_{ij} p_i^{(n)} p_j^{(n)}}{1 + J_{ij} p_i^* p_j^*} \quad (\text{S25a})$$

$$\langle \bar{a}_n \bar{a}_m \rangle_J \approx \langle \bar{a}_n \bar{a}_m \rangle_h \cdot \frac{1 + J_{ij} p_i^{(nm)} p_j^{(nm)}}{1 + J_{ij} p_i^* p_j^*}, \quad (\text{S25b})$$

where

$$p_i^{(n)} \equiv \langle c_i \rangle_{h^{(n)}} = p_i^* (1 - \hat{S}_{ni}) \quad (\text{S26a})$$

$$p_i^{(nm)} \equiv \langle c_i \rangle_{h^{(nm)}} = p_i^* (1 - \hat{S}_{ni})(1 - \hat{S}_{mi}). \quad (\text{S26b})$$

Expanding the fractions, we obtain

$$\langle \bar{a}_n \rangle_J \approx \langle \bar{a}_n \rangle_h (1 + J_{ij} p_i^{(n)} p_j^{(n)} - J_{ij} p_i^* p_j^*) \quad (\text{S27a})$$

$$\langle \bar{a}_n \bar{a}_m \rangle_J \approx \langle \bar{a}_n \bar{a}_m \rangle_h (1 + J_{ij} p_i^{(nm)} p_j^{(nm)} - J_{ij} p_i^* p_j^*). \quad (\text{S27b})$$

Substituting Eqs. S26, this becomes

$$\begin{aligned} \langle a_n \rangle_J &\approx \langle a_n \rangle_h + (1 - \langle \bar{a}_n \rangle_h) (\hat{S}_{ni} + \hat{S}_{nj} - \hat{S}_{ni} \hat{S}_{nj}) J_{ij} p_i^* p_j^* \\ &= \langle a_n \rangle_h + (1 - \langle a_n \rangle_h) (\hat{S}_{ni} + \hat{S}_{nj} - \hat{S}_{ni} \hat{S}_{nj}) \frac{p_{ij}}{2 p_i^* p_j^*}, \end{aligned} \quad (\text{S28})$$

where in the last expression the \bar{p}_i^* can also be replaced by \bar{p}_i to first order in J_{ij} . For the simple case of a random, binary sensitivity matrix with sparsity ξ , we obtain

$$\langle a_n \rangle_J \approx \langle a_n \rangle_h + p_{ij} (1 - \langle a_n \rangle_h) \left(\xi - \frac{\xi^2}{2} \right). \quad (\text{S29})$$

In the case where the correlations are predominately positive ($p_{ij} > 0$), the frequency of individual ligands and the receptor response are increased, $p_i > p_i^*$ and $\langle a_n \rangle_J > \langle a_n \rangle_h$, respectively. Consequently, the optimal sparsity must be smaller than in the uncorrelated case to have $\langle a_n \rangle_J = \frac{1}{2}$.

B. Continuous mixtures

We next consider mixtures where the concentrations of the individual ligands are drawn from a continuous distribution. For simplicity, we consider uncorrelated mixtures ($J_{ij} = 0$, $p_{ij} = 0$ for $i \neq j$), which are characterized by the probabilities p_i . In the case where receptors are excited by many ligands, the dot product $e_n = S_{ni} c_i$ can be approximated by another log-normal distribution [28], which is parameterized by the mean and variance given

in Eqs. 6. The survival function of the log-normal distribution then implies

$$\langle a_n \rangle \approx \frac{1}{2} \operatorname{erfc} \left[\frac{\ln \left(\frac{\sqrt{\langle e_n \rangle_c^2 + \operatorname{var}_c(e_n)}}{\langle e_n \rangle_c} \right)}{\sqrt{2 \ln \left(\frac{\operatorname{var}_c(e_n)}{\langle e_n \rangle_c^2} + 1 \right)}} \right]. \quad (\text{S30})$$

Since $a_n^2 = a_n$, the associated variance reads

$$\operatorname{var}(a_n) = \langle a_n \rangle (1 - \langle a_n \rangle), \quad (\text{S31})$$

which also determines the diagonal values of the covariance matrix $\operatorname{cov}(a_n, a_m)$. For $n \neq m$, we have

$$\langle a_n a_m \rangle = \int_1^\infty \int_1^\infty P_e(e_n, e_m) de_n de_m, \quad (\text{S32})$$

where $P_e(e_n, e_m)$ is the multivariate distribution of the two excitations e_n and e_m . We approximate $P_e(e_n, e_m)$ by a normal distribution, which describes the excitations e_n and e_m in the vicinity of $\langle a_n \rangle = \langle a_m \rangle = \frac{1}{2}$. This distribution is characterized by the means $\langle e_n \rangle$ together with the covariances $\operatorname{cov}(e_n, e_m)$, which comprise five parameters in total. Hence,

$$\begin{aligned} \langle a_n a_m \rangle &\approx \frac{1}{4} + \frac{1}{\sqrt{8\pi}} \left(\frac{\langle e_n \rangle - 1}{\sqrt{\operatorname{var}(e_n)}} + \frac{\langle e_m \rangle - 1}{\sqrt{\operatorname{var}(e_m)}} \right) \\ &\quad + \frac{(\langle e_n \rangle - 1)(\langle e_m \rangle - 1) + \operatorname{cov}(e_n, e_m)}{2\pi \sqrt{\operatorname{var}(e_n) \operatorname{var}(e_m)}} \end{aligned} \quad (\text{S33})$$

for $n \neq m$. The associated covariance $\operatorname{cov}(a_n, a_m)$ follows from the definition $\operatorname{cov}(a_n, a_m) = \langle a_n a_m \rangle - \langle a_n \rangle \langle a_m \rangle$, where we obtain the mean $\langle a_n \rangle$ by expanding Eq. S30 around the optimal point $\langle e_n \rangle = 1$ for small $\operatorname{var}(e_n)$,

$$\langle a_n \rangle \approx \frac{1}{2} + \frac{\langle e_n \rangle - 1}{\sqrt{2\pi \operatorname{var}(e_n)}}, \quad (\text{S34})$$

which is the same approximation that also led to Eq. S33. Consequently, we have

$$\operatorname{cov}(a_n, a_m) \approx \begin{cases} \frac{1}{4} - \frac{(\langle e_n \rangle - 1)^2}{2\pi \operatorname{var}(e_n)} & n = m \\ \frac{\operatorname{cov}(e_n, e_m)}{2\pi \sqrt{\operatorname{var}(e_n) \operatorname{var}(e_m)}} & n \neq m \end{cases}. \quad (\text{S35})$$

The conditions for optimal sensitivity matrices, $\langle a_n \rangle = \frac{1}{2}$ and $\operatorname{cov}(a_n, a_m) = 0$, can thus be expressed as

$$\langle e_n \rangle^4 = \langle e_n \rangle^2 + \operatorname{var}(e_n) \quad (\text{S36a})$$

$$\operatorname{cov}(e_n, e_m) = 0, \quad (\text{S36b})$$

see Eqs. S30 and S35. For small $\operatorname{var}(e_n)$, this reduces to $\langle e_n \rangle \approx 1$, which indeed leads to $\langle a_n \rangle = \frac{1}{2}$ in the approximation given in Eq. S34.

C. Numerical simulations

We use a simple two-step procedure to draw odors \mathbf{c} from the statistics $P_{\text{env}}(\mathbf{c})$. First, we determine the ligands that appear in a given mixture by drawing a random binary vector $\mathbf{b} = (b_1, b_2, \dots, b_{N_l})$ with $b_i \in \{0, 1\}$ from

$$P_{\text{cor}}(\mathbf{b}) = \frac{1}{Z} \exp(J_{ij} b_i b_j + h_i b_i), \quad (\text{S37})$$

analogously to Eq. S5. Here, h_i and J_{ij} determine p_i and p_{ij} according to Eq. S20 and Eq. S22, respectively. If ligand i appears in a mixture, i.e. if $b_i = 1$, its concentration c_i is drawn from a log-normal distribution with mean μ_i and standard deviation σ_i .

Given this odor statistics $P_{\text{env}}(\mathbf{c})$ and a sensitivity matrix S_{ni} , the mutual information I can in principle be calculated from Eqs. 1–3 of the main text. Calculating $P(\mathbf{a})$ to evaluate Eq. 3 involves an integral over $P_{\text{env}}(\mathbf{c})$ over the non-linear function given in Eq. 2. We approximate this integral using Monte Carlo sampling of the odor statistics $P_{\text{env}}(\mathbf{c})$. Because of the stochastic nature of Monte Carlo sampling, the calculated I is not exact. Consequently, we use the stochastic, derivative-free numerical optimization method CMA-ES [44] to optimize the sensitivity matrix S_{ni} with respect to I to produce Fig. 3B of the main text.

S3. PROPERTIES OF ARRAYS WITH RANDOM SENSITIVITIES

We study properties of receptors arrays characterized by random sensitivity matrices S_{ni} whose entries are independent and identically distributed. Here, we consider a log-normal distribution for the sensitivities, whose probability density function $f_S(S)$ and cumulative distribution function $F_S(S)$ read

$$f_S(S) = \frac{1}{\sqrt{2\pi}S\lambda} \exp\left[-\frac{1}{2\lambda^2} \left(\ln \frac{S}{\bar{S}} + \frac{\lambda^2}{2}\right)^2\right] \quad (\text{S38a})$$

$$F_S(S) = \frac{1}{2} \operatorname{erfc}\left[-\frac{1}{\sqrt{2}\lambda} \left(\ln \frac{S}{\bar{S}} + \frac{\lambda^2}{2}\right)\right] \quad (\text{S38b})$$

and are parameterized by the mean \bar{S} and the width λ , which is the standard deviation of the underlying normal distribution. Note that all following calculations could also be performed for other sensitivity distributions.

A. Concentration resolution

The fraction $\Phi_1(c)$ of receptors that are activated by a single ligand at concentration c reads

$$\Phi_1(c) = 1 - F_S(c^{-1}). \quad (\text{S39})$$

The typical concentration change δc that is necessary to excite η additional receptor is then defined by the condition $\Phi_1(c+\delta c) - \Phi_1(c) = \eta N_r^{-1}$. Expanding Φ_1 around c , the solution for δc reads

$$\delta c(c) = \frac{\eta}{N_r \Phi_1'(c)} = \frac{\eta c^2}{N_r F_S'(c^{-1})}. \quad (\text{S40})$$

For log-normal distributed sensitivities, the maximum of the associated resolution $R = c/\delta c$ is given in Eq. 10 of the main text.

B. Concentration range

The minimal concentration c_{\min} that can be sensed is defined by the condition $\Phi_1(c_{\min}) = \eta/N_r$, while c_{\max} is given by $\Phi_1(c_{\max}) = 1 - \eta/N_r$. Solving these equations, the concentration range $\zeta = c_{\max}/c_{\min}$ becomes

$$\zeta = \frac{G_S(1 - \frac{\eta}{N_r})}{G_S(\frac{\eta}{N_r})}, \quad (\text{S41})$$

where $G_S(y)$ is the inverse function of the cumulative distribution function $F_S(x)$. For log-normal distributed sensitivities, we obtain Eq. 11 of the main text.

C. Maximal number of distinguishable ligands

In the simple case of a mixture with s ligands, all at concentration c , the fraction $\Phi_s(c)$ of excited receptors is given by

$$\Phi_s(c) = 1 - \hat{F}_S(c^{-1}; s), \quad (\text{S42})$$

where $\hat{F}_S(z_n; s)$ is the cumulative probability function of the sum $z_n = \sum_{i=1}^s S_{ni}$. If the S_{ni} are log-normal distributed, the distribution for z_n can also be approximated by a log-normal distribution [28], which has mean $s\langle S_{ni} \rangle$ and variance $s \operatorname{var}(S_{ni})$. In this case,

$$\Phi_s(c) = 1 - \frac{1}{2} \operatorname{erfc}\left[\frac{\ln\left(\frac{c\bar{S}s^2}{\sqrt{s(r+s)}}\right)}{\sqrt{2\ln\left(\frac{r+s}{s}\right)}}\right] \quad (\text{S43})$$

where $r = \bar{S}^{-2} \operatorname{var}(S) = \exp(\lambda^2) - 1$ is the squared coefficient of variation. Fig. S1A shows that Eq. S43 approximates the numerically determined $\Phi_s(c)$ well.

We next consider the maximal number of ligands that can be distinguished. Here, we for simplicity consider the case where mixtures can be distinguished when they excite activity patterns that differ for at least η receptors. Since a mixture with s components on average excites $N_r \Phi_s$ receptors, this condition reads

$$N_r \Phi_{s+1}(c) \geq N_r \Phi_s(c) + \eta. \quad (\text{S44})$$

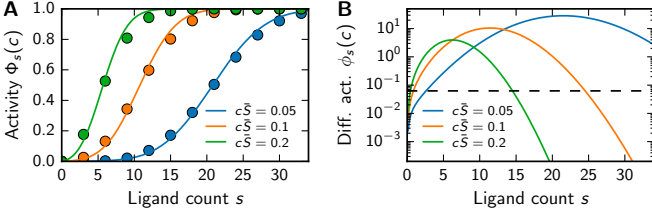


FIG. S1: Receptors are most sensitive to mixtures of medium size. (A) $\Phi_s(c)$ as a function of s for various c at $\lambda = 1$. Eq. S43 (solid lines) is compared to numerical simulations (symbols). (B) $\phi_s = d\Phi_s/ds$ as a function of s for various c at $\lambda = 1$. The dashed line marks the threshold N_r^{-1} below which mixtures are not distinguishable for $N_r = 300$.

Expanding $\Phi_s(c)$ as a function of s , this condition can be approximated by

$$\phi_s(c) \geq \frac{\eta}{N_r}, \quad (\text{S45})$$

where $\phi_s(c) = d\Phi_s(c)/ds$. Fig. S1B shows that this function has a single peak. Mixtures with $s = 0, \dots, s_*$ ligands can thus all be distinguished from each other if

$$\phi_1(c) \geq \frac{\eta}{N_r} \quad \text{and} \quad \phi_{s^*}(c) \geq \frac{\eta}{N_r}. \quad (\text{S46})$$

Here, the first condition ensures that c is above the odor detection threshold, while the second condition ensures that the two largest mixtures excite sufficiently different activity patterns.

D. Discriminability of two mixtures of equal size

We next consider how well two mixtures can be discriminated. For simplicity, we consider two mixtures with each s ligands of which s_b are shared. We call these two mixtures plus (+) and minus (−) to distinguish them. To determine the Hamming distance between the activation patterns, we first consider the excitations e_{\pm} of a single receptor caused by the two mixtures,

$$e_{\pm} = \sum_{i \in \mathcal{C}_b} S_{ni}c + \sum_{i \in \mathcal{C}_{\pm}} S_{ni}c. \quad (\text{S47a})$$

Here, \mathcal{C}_b denotes the set of ligands appearing in both mixtures, while \mathcal{C}_{\pm} denote those only appearing in either of the mixtures. Note that we only consider the case where the ligands appear with the same concentration c . The excitations can be rewritten as

$$e_{\pm} = (z_b + z_{\pm})c \quad (\text{S48})$$

where the z_x are random variables. Here, z_b is distributed according to $\hat{F}_S(z; s_b)$, while z_{\pm} are distributed according to $\hat{F}_S(z; s - s_b)$. The probability p_s that the receptor activity is the same for both mixtures is given by

$$p_s = P(e_+ < 1 \wedge e_- < 1) + P(e_+ > 1 \wedge e_- > 1). \quad (\text{S49})$$

The first term can be expressed as

$$P(e_+ < 1 \wedge e_- < 1) = \int_0^{\frac{1}{c}} dz_b \hat{f}_S(z_b; s_b) \cdot \int_0^{\frac{1}{c} - z_b} dz_+ \hat{f}_S(z_+; s_d) \int_0^{\frac{1}{c} - z_b} dz_- \hat{f}_S(z_-; s_d), \quad (\text{S50})$$

where $s_d = s - s_b$ is the number of ligands that are differ between the two mixtures. Here, $\hat{f}_S(z; s)$ denotes the probability density functions of $\hat{F}_S(z; s)$. Eq. S50 can also be written as

$$P(e_+ < 1 \wedge e_- < 1) = \int_0^{\frac{1}{c}} dz_b \hat{f}_S(z_b; s_b) \left[\hat{F}_S\left(\frac{1}{c} - z_b; s_d\right) \right]^2. \quad (\text{S51})$$

Similarly, the second term in Eq. S49 can be expressed as

$$P(e_+ > 1 \wedge e_- > 1) = 1 - \hat{F}_S\left(\frac{1}{c}; s_b\right) + \int_0^{\frac{1}{c}} dz_b \hat{f}_S(z_b; s_b) \left[1 - \hat{F}_S\left(\frac{1}{c} - z_b; s_d\right) \right]^2, \quad (\text{S52})$$

where the first term is the probability that the ligands appearing in both mixtures excite the receptor alone. The second term denotes the probability that although z_b is not large enough, both z_+ and z_- are sufficient to bring the excitation above threshold. The mean Hamming distance $h = N_r(1 - p_s)$ between the activation patterns of the two mixtures then reads

$$h = 2N_r \int_0^{\frac{1}{c}} \hat{f}_S\left(\frac{1}{c} - z; s_b\right) \hat{F}_S(z; s_d) [1 - \hat{F}_S(z; s_d)] dz. \quad (\text{S53})$$

To test this equation, we randomly draw mixtures at given s and s_b , determine their activation pattern according to Eqs. 1–2, and determined the associated difference. Fig. S2 shows that Eq. S53 agrees well with these numerical results. Although h is a function of s , s_b , c , \bar{S} , λ , and N_r , the only important parameters are s , s_b , $c\bar{S}$, and λ , since N_r is just a prefactor and \bar{S} only sets the scale of typical concentrations. We can thus explore the behavior by plotting h as a function of s and $c\bar{S}$ for different s_b , see Fig. S3. This plot shows that mixtures can be distinguished well when the concentration is in the right interval. Fig. S3 can be used to determine the parameter region in which a receptor array is likely able to distinguish two mixtures. In the simple case where the activity patterns must be different in at least η receptors, mixtures can typically be distinguished if $h > \eta$.

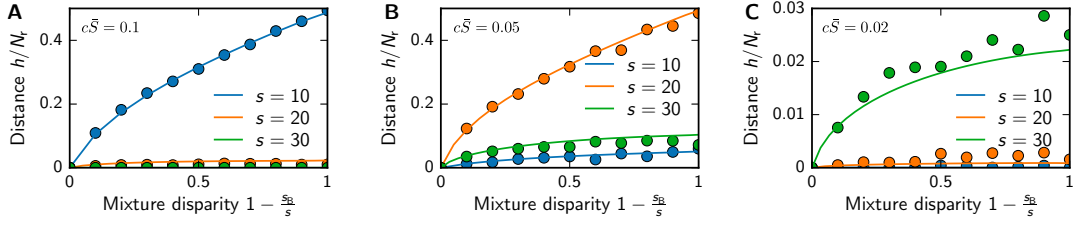


FIG. S2: Mean normalized mixture distance h/N_r as a function of the mixture disparity $1 - s_b/s$ for $\lambda = 1$, various mixture sizes s , and (A) $c\bar{S} = 0.1$, (B) $c\bar{S} = 0.05$, (C) $c\bar{S} = 0.02$. The analytical result given in Eq. S53 (solid lines) is compared to numerical simulations (symbols).

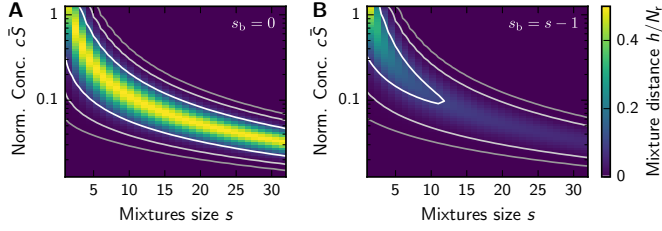


FIG. S3: Mean normalized mixture distance h/N_r from Eq. S53 as a function of mixture size s and concentration c of the ligands for $\lambda = 1$ and (A) $s_b = 0$, (B) $s_b = s - 1$. The lines indicate iso-contours at $h/N_r = 0.1, 0.01, 0.001$ (white to gray).